



1994

# Ignition and Environmental Effects of Wildfires as Related to Giant Impacts

Gregory S. Kufner '94

*Illinois Wesleyan University*

---

## Recommended Citation

Kufner '94, Gregory S., "Ignition and Environmental Effects of Wildfires as Related to Giant Impacts" (1994). *Honors Projects*. Paper 17.

[http://digitalcommons.iwu.edu/chem\\_honproj/17](http://digitalcommons.iwu.edu/chem_honproj/17)

This Article is brought to you for free and open access by The Ames Library, the Andrew W. Mellon Center for Curricular and Faculty Development, the Office of the Provost and the Office of the President. It has been accepted for inclusion in Digital Commons @ IWU by the faculty at Illinois Wesleyan University. For more information, please contact [digitalcommons@iwu.edu](mailto:digitalcommons@iwu.edu).

©Copyright is owned by the author of this document.

**IGNITION AND ENVIRONMENTAL  
EFFECTS OF WILDFIRES AS  
RELATED TO GIANT IMPACTS**

Gregory S. Kufner

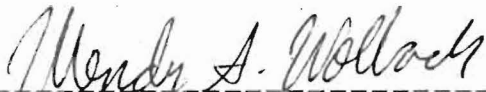
Approval Page

Ignition and Environmental Effects of Wildfires as Related to Giant  
Impacts

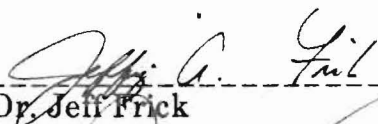
Gregory S. Kufner

A PAPER SUBMITTED IN PARTIAL FULFILLMENT OF THE  
REQUIREMENTS FOR CHEMISTRY 499 AND HONORS IN CHEMISTRY.

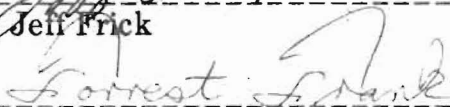
Approved, Honors Committee:



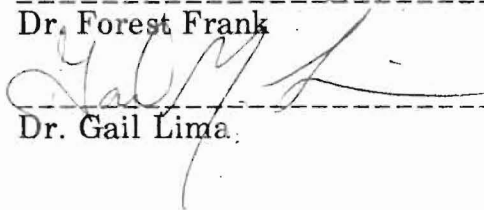
-----  
Dr. Wendy S. Wolbach, project advisor



-----  
Dr. Jeff Frick



-----  
Dr. Forest Frank



-----  
Dr. Gail Lima

Illinois Wesleyan University  
1994

## **Acknowledgements**

I would like to thank Vanya Petrov and Irena Dumar at the University of Illinois for their assistance with the SEM. I would also like to thank Dr. Wendy S. Wolbach for her ideas and her help with this project.

## Abstract

Soot has been discovered by Wolbach *et al.* at the Cretaceous-Tertiary boundary in various geographic locations, supporting the theory that worldwide wildfires were ignited by the impact of a giant meteorite which caused the mass extinction 65 million years ago. This project examines a deep sea core sample from the North Central Pacific Ocean for evidence of soot. Soot discovery at this site, the only deep ocean site to be studied, supports the theory that soot distribution from the fires was worldwide.

In another project, samples from the suevite breccia of the Kara Ust-Kara craters in Russia (unrelated to the KT impact) were examined for soot to find evidence of fires triggered by a different impact. After demineralization to remove the minerals in the rock, reduced carbon was found in both the core and crater samples. Oxidation in dichromate solution removed the organic carbon (kerogen) from the samples. Analysis of the post-oxidation residues under a scanning electron microscope confirmed the presence of soot in both the core and crater samples.

## Introduction

In 1980, Luis Alvarez and his coauthors proposed the theory that the extinction at the Cretaceous-Tertiary boundary (KTB), 65 million years ago, was caused by the impact of a large meteorite. Originally they had looked at the iridium content in the clay at the interface between Cretaceous and Tertiary sediments (the Cretaceous-Tertiary boundary) at various different geographic locations in order to determine the length of time it took for the clay to form. They assumed that if the rate at which iridium fell from micrometeorites was constant, they could obtain the rate at which the sedimentation occurred [Alvarez, 1986]. Iridium was used as a marker because the concentration of terrestrial iridium is very low in the earth's crust. Most of the iridium that exists in the earth is concentrated in the core, while the concentration of iridium in extra-terrestrial materials, such as asteroids, is much higher and more uniformly spread through the object (on the order of 0.5 ppm for a type I carbonaceous chondrite meteorite vs. 0.1 ppb in the earth's crust [Alvarez *et al.*, 1980]). Neutron activation analysis of samples from Gubbio, Italy, yielded an iridium content in the KTB of  $\approx 5.5$  ppb, thirty times greater than the 0.3 ppb found above and below it [Alvarez *et al.*, 1980]. Samples from Højerp Church, Denmark, were also examined. Iridium content at the boundary was determined to be 41.6 ppb, about 160 times greater than the baseline values of about 0.26 ppb [Alvarez *et al.*, 1980]. Since an iridium concentration of 0.1 ppb is assumed for the earth's crust, an average abundance of 6.3 ppb cannot be explained by normal (surface) terrestrial sources [Alvarez *et al.*, 1980].

Volcanic eruptions could produce the required concentration, however worldwide distribution would be a problem. Additionally, tektites (glassy fragments) were found in the KT boundary clay [Smit and Klaver, 1981]. Unlike the angular tektites that would be found in the violent eruption needed to produce the chance of worldwide distribution of the fragments, the microtektites found at the boundary were spherules characteristic of molten droplets which were cooled through the upper atmosphere and re-heated upon re-entry [Alvarez, 1986]. These spherules are characteristic of impacts as glass is formed from silicate rock by the extreme release of heat and energy of an impact.

Shocked quartz was found to be present in the KTB by Bruce Bohor [Bohor et al., 1984]. Quartz grains which contain stress and shear lines as a result of tremendous sudden forces are termed shocked. Forces on the order of impacts and nuclear blasts are needed to produce these effects; a volcanic eruption could not [Alvarez, 1986].

Since terrestrial processes have been ruled out, an extraterrestrial source for the iridium was the only remaining possibility. Extraterrestrial materials, such as meteorites, have been known to contain iridium at concentrations at hundreds of parts per billion. Due to the lack of the heavy element  $^{244}\text{Pu}$ , a supernova explosion which could have produced the observed Ir concentration was eliminated as a possible cause of the KT extinctions since  $^{244}\text{Pu}$  would have been produced as well in such an explosion. Alvarez et al. (1980) then postulated that a  $10 \pm 4$  km meteorite impact could have produced the observed iridium concentration.

The size of the meteorite was calculated by comparing the known Ir abundance in a meteorite with the observed iridium concentration over the entire planet. Samples with high Ir concentration from geographically diverse sites such as Gubbio Italy, Højerup Church Denmark, and Woodside Creek, New Zealand lend credibility to the theory of worldwide distribution of Ir [Alvarez et al., 1980]. Today over 75 different sites with high Ir concentrations are known [Alvarez et al., 1986]. The mass of the asteroid was then calculated using the expression:

$$M = sA/f$$

where  $M$  is the mass of the meteorite,  $s$  is the surface density of the Ir,  $A$  is the surface area of the earth, and  $f$  is the fractional abundance of Ir in a type I carbonaceous chondrite asteroid, which are considered typical of solar system material [Alvarez et al. 1980].

Assuming that a 10 km meteorite did in fact impact upon the earth, 65 million years ago, McLaren et al. (1990) modeled the effects that such an impact would cause. Based upon the assumption that the meteorite travelled at 20 km/s and that the impact occurred in a shallow sea near the Yucatan Peninsula, the energy

released by the impact was equivalent to  $6.2 \times 10^7$  megatons of TNT. This massive release of energy is greater than the energy that would be released if all of the nuclear weapons on the planet were exploded simultaneously [McLaren et al. 1990].

Upon impact, a blast wave of superheated air at a temperature of approximately 20,000 K would form. The heat and high winds from the blast wave could dry out trees and start massive wildfires globally. Since the impact took place in the sea floor, a large tsunami would form and scour the ocean floor. The impact would produce an earthquake with a magnitude of 12.4 on the Richter scale (an earthquake with a magnitude greater than 8.9, the highest recorded by man) which would increase existing volcanic activity. A crater on the order of 100 km could result from an impact of this magnitude [Alvarez, 1986]. Over one hundred  $\text{km}^3$  of terrestrial rock and  $9 \times 10^{13}$  tons of vaporized meteorite would be ejected into the upper atmosphere with 10-20% of the material being distributed worldwide over several months before settling out [McLaren et al., 1990]. This material would cause global cooling and darkness, stop photosynthesis, and disrupt the food chain. Additionally, rapid heating of the atmosphere before and after impact could produce great quantities of nitrous and nitric acid which would attack the ozone layer, and cause acid rain which would further defoliate the land.

The extreme heat created in the fireball could start wildfires on continents  $10^3$  km away from the impact center [Wolbach et al., 1985]. The high winds would also aid in world-wide distribution of soot from the fires. Wolbach, Lewis and Anders (1985) discovered traces of elemental carbon and soot during the search for noble gases that would have been present in the meteorite. Deposition of soot and elemental carbon signified that fires must have taken place at the time of the boundary. Samples from Denmark, New Zealand, and Spain were all found to contain on the average 5033 ppm of elemental carbon. This average divided by the surface area of the earth represents a surface abundance of  $0.021 \text{ g/cm}^2$ , a quantity representing 4 percent of the total assumed biomass of carbon ( $0.5 \text{ g/cm}^2$ ) during that time period [Wolbach et al., 1985]. This shows the massive extent of the wildfires generated by the impact.



In the atmosphere, the high concentration of soot prior to its deposition in the oceans as part of the accumulating sediment, would contribute to the absorption of sunlight, since soot absorbs light better than rock ejecta due to the higher optical depth (ability to absorb) of soot. Additionally carbon monoxide which would have been produced by such global fires would have aided in the extinction process. Carbon dioxide and water produced in the combustion process and the oceanic impact would have later exacerbated the greenhouse effect which could have increased global temperatures by about 17°C [Wolbach et al., 1988]. All of these factors support the contribution of global fires to the environmental changes which resulted in the mass extinction event 65 million years ago.

### **This Investigation**

This study consisted of two different but related projects. First, a deep sea core from the DSDP site 465A in the North Central Pacific Ocean was examined for elemental carbon, in an attempt to verify the global distribution of soot particles. The single previous deep core studied by Wolbach gave less than 3 ppm carbon [Wolbach et al., 1990]. This lack of carbon could have been due to an oxidizing oceanic environment. DSDP 465A is an undisturbed core with a sharp, dark KTB, and comes from a reducing oceanic environment. A reducing environment should have preserved the carbon in the KTB. If soot is found, the theory of worldwide distribution of soot will gain additional support. If absent, previously discovered soot might be re-interpreted as a more local phenomenon, perhaps concentrated in continental margins due to runoff from land (all samples where soot was found in abundance were continental margins 65 million years ago).

For this study, a single 2 cm clast (or small fragment) was obtained from the drill core and part of this clast was analyzed. Samples from below and above the KTB (the Cretaceous and Tertiary) at the same site were also examined for baseline comparison.

The second part of the project was the analysis of a series of unrelated samples from the Kara and Ust-Kara impact craters in Russia. The Kara and Ust-Kara craters in Russia are twin craters formed most likely by the simultaneous impact of two large bodies.

Sometimes when a large meteorite enters the atmosphere, forces and heating due to entry into the atmosphere separate one large body into two. These craters were probably formed by such an event. Evidence for this exists in the twin craters that can be found on the moon.

The Kara crater with a diameter of 66 km and the Ust-Kara crater with an average diameter of 75 km are thought to have been caused by a split meteorite with a total estimated mass of  $5.5 \times 10^{13}$  kg [Masaitis et al., 1988] which impacted in the shallow Kara sea. Had this body been a single impact, a crater of 88 km diameter could have formed [Masaitis et al., 1988], perhaps causing yet another extinction event. Since the meteorite split upon entry, the release in energy was not as great as that of the larger, single meteorite which caused the KTB extinction. According to paleontological [Alekseev et al., 1988],  $^{40}\text{Ar}$ - $^{39}\text{Ar}$  [Nazarov et al., 1988], and paleomagnetic dating techniques [Badjukov et al., 1988] which were performed, an age of 74-75 million years was determined for this impact event.

Argon dating techniques are possible due to small amounts of the inert gas Ar in various isotopes which decay at a set rate. Since the half life of the radioactive isotope is known, the time of capture of the gas can be determine, determining the age of the rock. This places the impacts about ten million years before the K-T boundary event, which could correspond to the Campanian/Maastrichtian boundary which occurred around 74 Ma [Koeberl et al. 1990].

These samples are interesting because they might offer independent confirmation of soot formation tied to an impact. Analysis of this site is also interesting due to the rarity of twin impact craters of this size on the earth [Koeberl et al. 1990].

The seven samples analyzed were collected in the Kara crater at the Saayakha River where the upper part of a suevite breccia and its overlying sediments are exposed. The suevite layer is formed of rocks composed of lithic and glass fragments with a matrix of crushed material and glass. Glasses can form due to the heat and pressure changes resulting from an impact. The ejecta is rapidly heated by the impact and cooled by the air as the ejecta settles, causing glass to form. The lithic fragments are composed of shales and sandstones. Because the impact occurred in a shallow sea, clast

and glass size vary with larger and heavier fragments on the bottom of the layer. This occurs due to differences in Stokes settling rates for different sized clasts.

Any soot would be expected in the overlying sediments closest to the top of the suevite layer, since soot particles should be the lightest of the particles found in the sedimentary rocks of the breccia and would have settled out later than the suevites. The suevites in these samples are rocks composed of Permian shales and sandstones, matrix (crushed material), and glass fragments.

The core samples were obtained from the KT boundary at DSDP Site 465. The core sample contains a dark boundary layer approximately 3 mm in thickness (Figure 2), an indication that carbon may be present in the layer. A portion of this sample (0.02899 g) was examined. Additionally, one sample from the Tertiary and the Cretaceous layers were taken from areas well above and below the boundary and analyzed. Both these samples were light colored in appearance, an indication that carbon could only be present in small quantities. Much of these two samples reacted with the 9 M HCl and dissolved rapidly.

The Kara Ust-Kara samples were originally large pieces of rock most over 2 cm in diameter. These samples were all a dark shade of grey. The samples were crushed to a powder and demineralized. Soot content in all of the samples was thought to be a possibility due to the dark grey coloration of all the samples.

Samples were obtained from 0.1, 10, 25, and 30 m below the top of the suevite breccia layer, and 2 cm, 1.5 m, and 2.4 m above this layer (Figure 1).

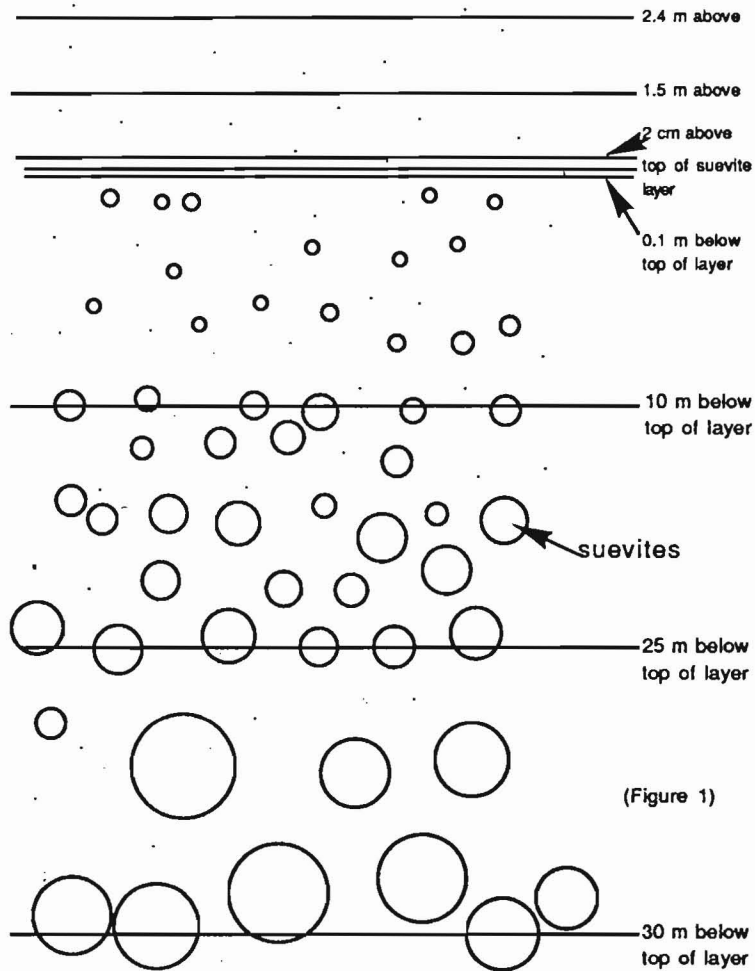


Figure 1. Diagram of the Kara Ust-Kara suevite breccia and overlying sediments with sample locations in relation to the top of the suevite breccia.

Any soot would be expected in the overlying sediments closest to the suevite layer, since soot particles should be the lightest of the particles found in the sedimentary rocks of the breccia and would have settled out later than the suevites. The suevites in these samples are rocks composed of Permian shales and sandstones, matrix (crushed material), and glass fragments.

CM 1 2 3 4 5

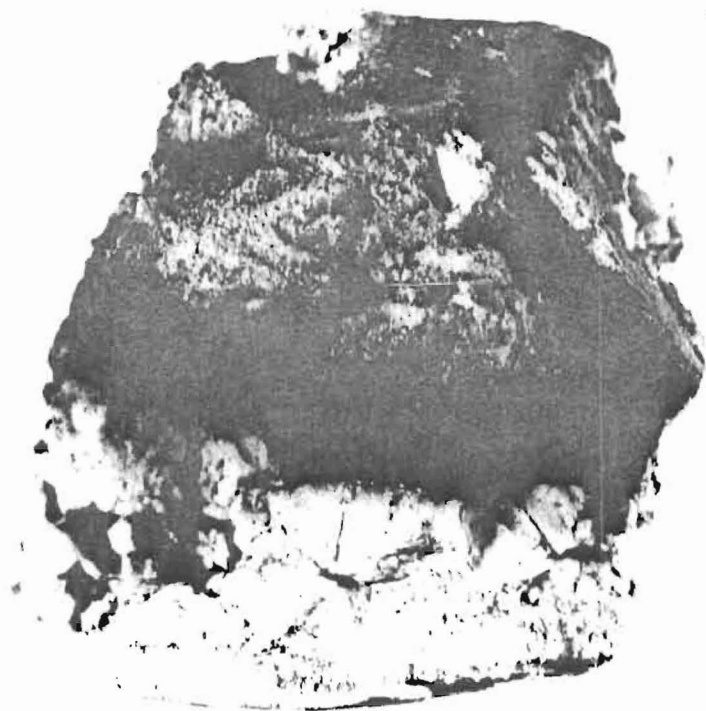
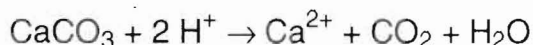
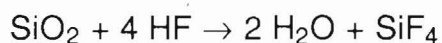


Figure 2. Deep sea core (KT boundary, sample KT).

Since isolation of elemental carbon was critical to both projects, all samples were analyzed in the same manner. They were pre-weighed and treated with HCl in order to remove all of the calcium carbonate via the following reaction:

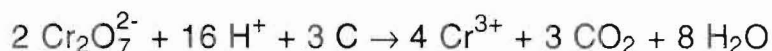


Following dissolution of  $\text{CaCO}_3$ ,  $\text{Ca}^{2+}$  and remaining  $\text{CO}_2$  was removed via copious rinsing with  $\text{H}_2\text{O}$  to prevent interference with subsequent steps. For example, calcium contamination would cause precipitation of  $\text{CaF}_2$  as HF is added. After rinsing, the samples were treated with HF/HCl in order to dissolve silicates via the general reaction:



The stoichiometric coefficients in the above reaction vary from sample to sample depending upon the composition of the silicate matrix. Rinsing then removed the remaining  $\text{SiF}_{4(g)}$  in the solution. Alternating treatments with HCl and HF/HCl completed the demineralization. Each primary carbonaceous residue was rinsed, dried and weighed. These residues were then oxidized with acidic dichromate to destroy organic carbon.

Following removal of mineral components, many KTB samples contain both organic carbon (kerogen) and elemental carbon (mainly soot and some charcoal). Isolation of elemental carbon required oxidizing the samples in acidic  $\text{Cr}_2\text{O}_7^{2-}$  solution at  $50^\circ\text{C}$ . A period of 600 hours destroyed most of the organic carbon via the reaction:



and left a residue of elemental carbon and trace amounts of other insoluble minerals such as rutile ( $\text{TiO}_2$ ).

Based on experiments performed by Wolbach *et al.* (1989) on Woodside Creek KT boundary clays, it was determined that the oxidation of carbonaceous residue by dichromate follows first order

kinetics and can be observed by plotting the mass fraction of carbon left vs the time of oxidation, into three components of half-lives of 610 hrs, 59 hrs, and 7 hrs (Figure 3. [Wolbach *et al.* 1989]). The long-lived component is elemental carbon both soot and charcoal. The short-lived component with a half-life of 7 hrs. is consistent with type I kerogen (chemically the least reduced). This kerogen forms a filmy coating on top of the soot molecules and is the first to be oxidized. The medium-lived components are Type II and Type III kerogens (more reduced). These half-life correlations were determined by separate oxidations of the kerogens, carbon black and charcoal. Charcoal and soot gave long half-lives greater than 800 hrs. Type III kerogen gave the longest half-life of 180 hrs. Carrying on a 600 hr oxidation destroys 99% of the kerogens while leaving approximately 50% of the elemental carbon [Wolbach *et al.* 1989].

The mass of the carbon after the 600 hour oxidation was compared to the mass of the original carbonaceous residue and the residue left after all carbon was completely oxidized (usually >1000 hr) in order to determine the quantity of elemental carbon and insoluble minerals, such as rutile, present in the sample. The 600 hr carbon sample was viewed using a scanning electron microscope for soot identification and has shown the characteristic morphology (grapelike clusters of particles) of soot in 11 of 12 of the geographically widespread sample sites analyzed [Wolbach *et al.*, 1989].



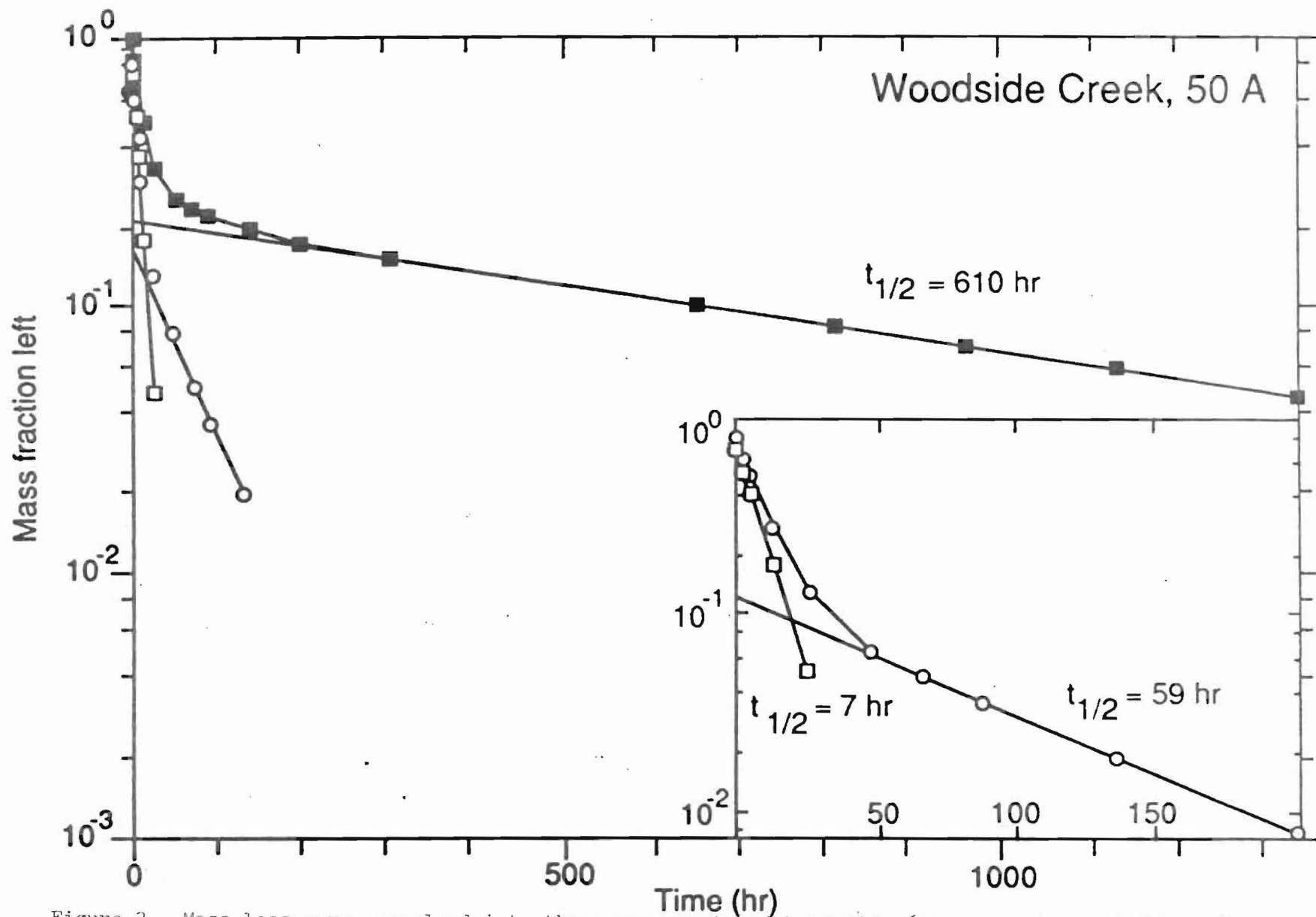


Figure 3. Mass loss curve resolved into three components of half-life 610 hr, 59 hr, and 7 hr. They apparently represent elemental C, resistant kerogen, and reactive kerogen (Wolbach *et al.* 1989).

## Procedure

All samples studied were crushed to a powder and treated with an excess of 9M HCl for about 24 hours in order to remove calcium carbonate from the sample. Samples were centrifuged and HCl was removed. Samples were then rinsed with distilled water in order to remove all  $\text{Ca}^{2+}$  from the samples. After several rinses, usually five or more, an excess of 10M HF/1M HCl was slowly added to the samples. The HF/HCl demineralized the samples leaving soot and rutile behind. The samples were rinsed several more times and a series of alternating HCl and HF/HCl treatments completed the demineralization.

The black residues were then dried and weighed. Samples were then suspended in 10 ml of 0.1M  $\text{Cr}_2\text{O}_7^{2-}$  in 2M  $\text{H}_2\text{SO}_4$  at 50°C for 600 hours in order to destroy all of the organic carbon. Elemental carbon, which is harder to oxidize, remained after the 600 hours. The level of the dichromate solution and the level of the water in the temperature bath were kept constant. Additionally, when the orange color of the dichromate solution began to turn green, indicating the accumulation of  $\text{Cr}^{3+}$ , the oxidation was stopped by a water rinse and fresh dichromate solution was added in order to keep the rate of oxidation roughly constant.

Sample KT was then analyzed using a Hitachi S800 Field Emission Hi Resolution Scanning Electron Microscope located at the University of Illinois. The sample was suspended in distilled water using an ultrasonic bath. A drop of the sample was then placed on carbon conductive tape, dried under a heat lamp and then in a vacuum, vacuum sputter coated with a gold-palladium film  $< 100 \text{ \AA}$  thick, placed in the SEM, and analyzed. Structures were found at magnifications greater than 20,000 times.

## Results from DSDP Core Samples

After the 600 hr oxidation of the core samples little residue remained (Table 1). Sample K50, the sample from the Cretaceous layer, contained no visible residue even under 400 times magnification under a light microscope. Sample T120, the Tertiary sample, also did not contain any visible residue. Sample KT, the Cretaceous-Tertiary boundary sample, contained a small amount of crystals that were only discernable under 400x magnification. These crystals appeared colorless, however the small amount of residue may have precluded the true determination of the color of the residue.

Weighing all three samples after rinsing and drying gave some erroneous results (see Table I).

Table I. Mass of deep sea core samples after 600 hr oxidation.

Sample Name	Mass before demineralization (g)	Mass of test tube w/o sample (g)	Mass of test tube w/ sample (g)	Mass of sample before oxidation (g)	Mass of sample after oxidation (g)
KT	0.02899	20.66373	20.66220	0.00250	-0.00153
K50	1.49786	19.84597	19.84561	0.00143	-0.00036
T120	1.74741	19.84994	19.85002	0.00059	0.00008

As can be seen from Table I, negative masses were obtained from two of the samples, including the KTB layer sample in which crystals had been previously observed. A study was then undertaken to try to determine the source of the errors.

First the balance, a Mettler A261, was recalibrated automatically and the tubes with samples reweighed. The weights did not fluctuate more than  $\pm 0.00005$  g. Therefore a manual calibration with two standard 100 g Mettler weights was performed and the samples reweighed. Again a  $\pm 0.00005$  fluctuation occurred. Additionally, other standard Mettler 100 g weights were measured after calibration and the weights were accurate to  $\pm 0.0001$  g.

Climate conditions were then examined. On drying, the samples became somewhat hygroscopic. Variations in humidity could have affected the weights. Weighing the samples dry produced only a  $\pm 0.1$  mg variation in the weight of the samples. Temperature fluctuations were also examined. A balance with a sensitivity of 0.01 mg is prone to air currents caused by temperature gradients in the atmosphere. These currents could "add" or "subtract" mass depending upon their direction. Placing the balance in a temperature and humidity controlled room had no substantial effect upon the masses other than the fact that the samples came to constant weight faster.

Finally, the mass of the ink marking the test tube was examined. A clean tube was massed, marked with a "KT" marking of approximately the same size as the original marking, allowed to dry overnight. The next day the tube was weighed and a value of 0.00002 g was obtained for the weight of the ink. All samples were handled using Kimwipes in order to prevent fingerprints from contributing to the weight of the tubes.

Taken together none of these errors can explain the error in the masses of the samples. It was assumed that the error came from the initial weighing of the test tubes before treatment with the dichromate. It was impossible to transfer the samples to another test tube in order to reweigh due to the mass loss which would likely have occurred during transfer.

Therefore a mass of 0.00001 g (the limit of the balance) was assumed for samples K50 and KT. The weights were then used to

calculate the upper limit concentration of soot in the sample (Table II).

Table II. Upper limit concentrations of soot in the core samples.

Sample	Upper limit concentration of soot (ppm)
K50	46
KT	344
T120	7

\*Concentrations good to one significant figure

As might be expected the boundary layer has the highest upper limit concentration of soot.

Under magnification with a SEM, several structures had cubic crystalline forms consistent with undissolved minerals. Other structures contained oddly shaped rounded clusters attached to larger smoother irregular surfaces. Micrographs of several of these structures were taken (Figures 4-11).

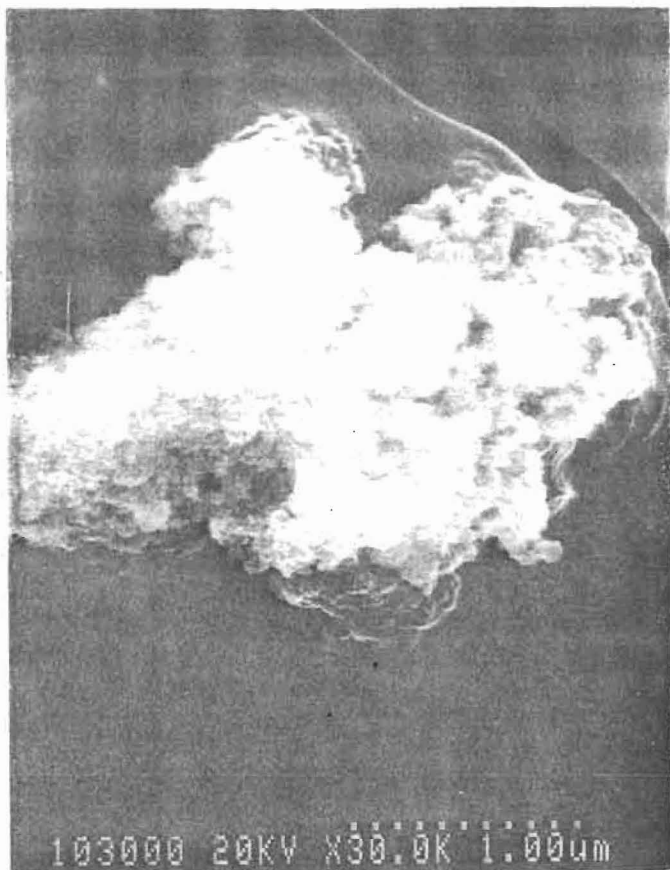


Figure 4. Sample KT. Charcoal with mineral embedded.

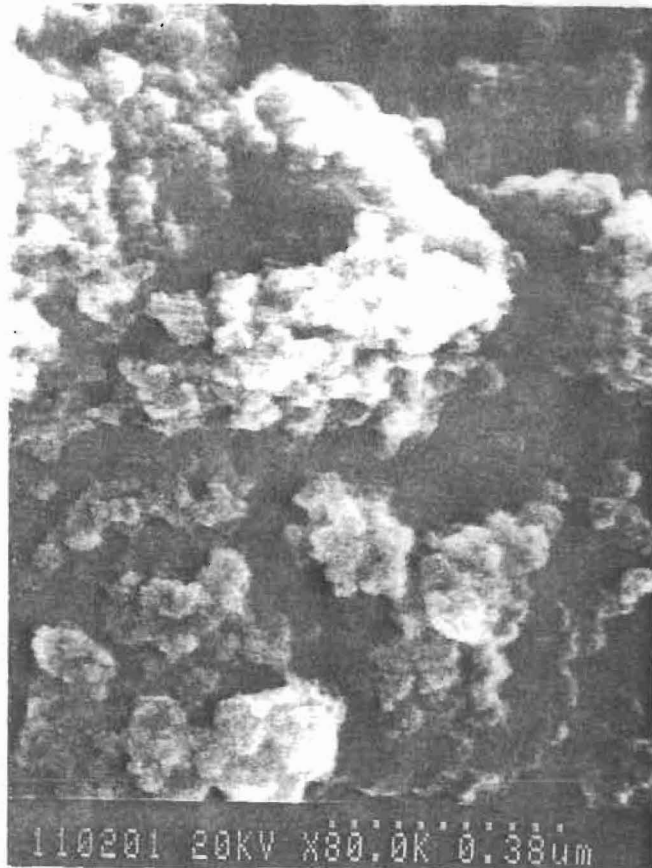


Figure 5. Close-up of mineral in Figure 4.

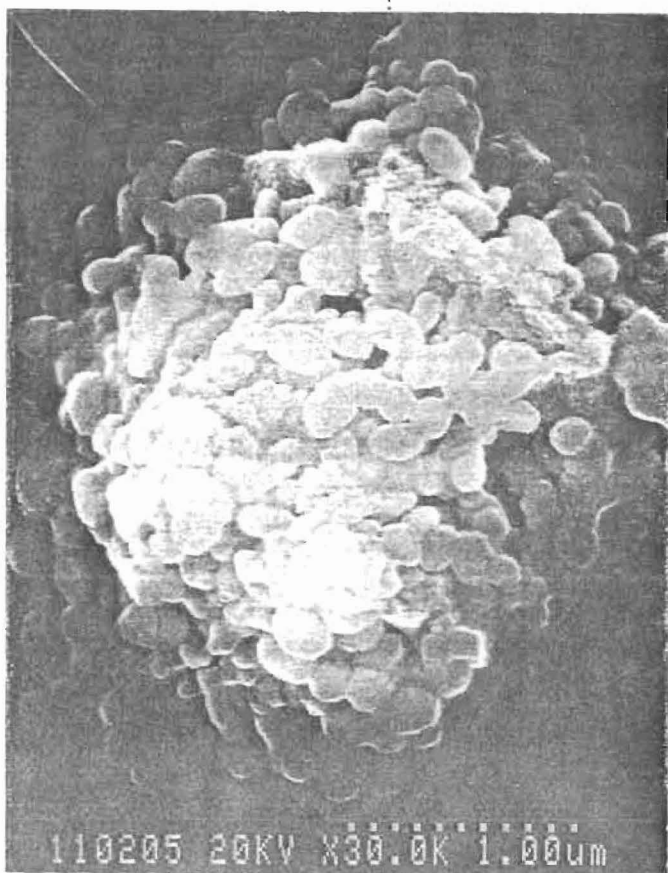


Figure 6. Charcoal with possible soot covering (Sample KT).

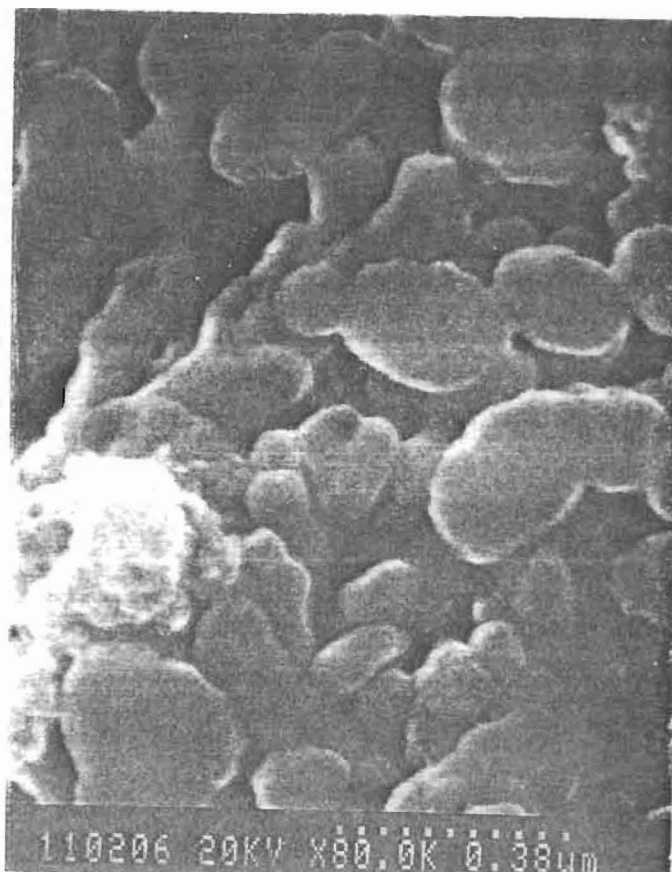


Figure 7. Close-up of Figure 6 surface.



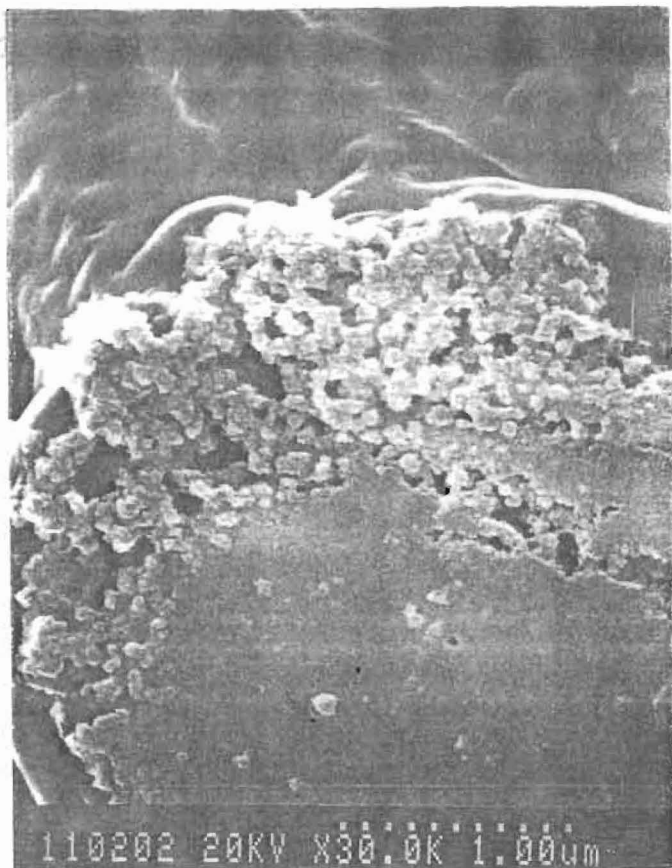


Figure 8. Soot particles attached to mineral of kerogen (Sample KT).

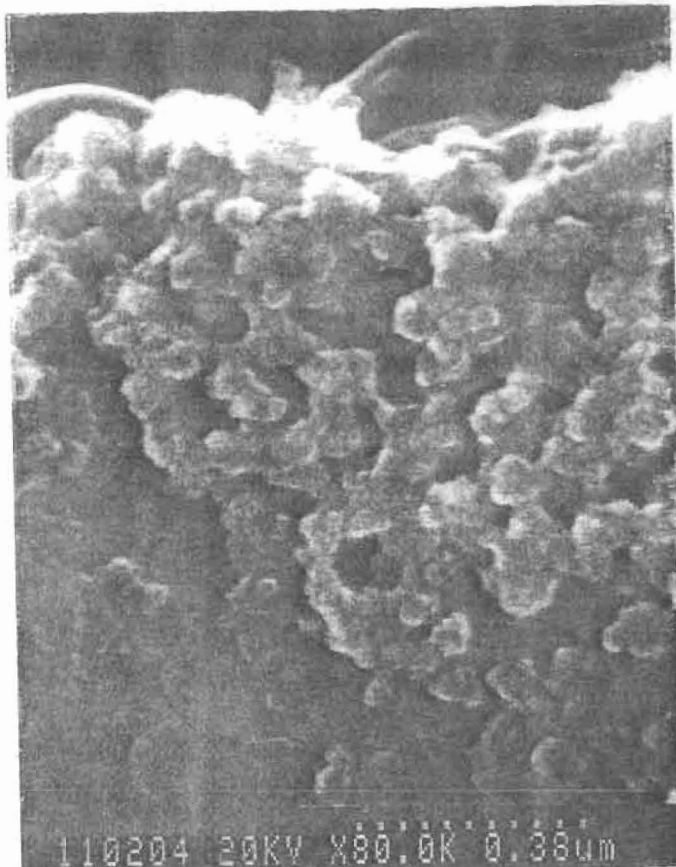


Figure 9. Close-up of soot in Figure 8.



Figure 10. Close-up of soot in Figure 8.

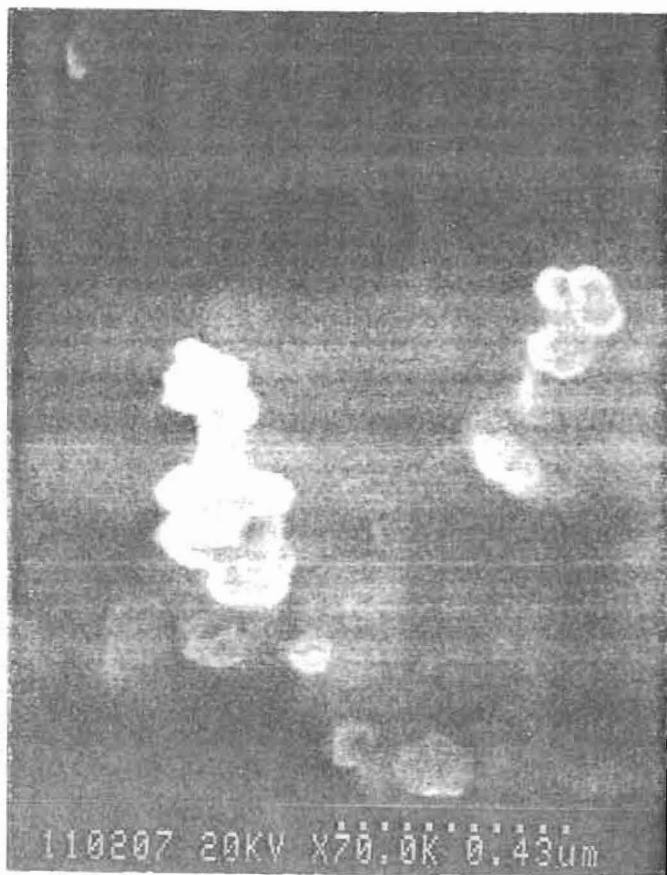


Figure 11. Isolated soot clusters (Sample KT).

Figures 4 and 5 show a large amorphous mass, possibly charcoal, in which is embedded a single large crystal of an undissolved mineral (possibly rutile). Unfortunately, elemental analysis was not carried out due to the type of conductive tape that was used. The carbon based tape would have hidden the carbon signal of the charcoal under a very large peak. [SEM work on the Kara Ust-Kara samples should have been carried out using a different type of tape so that elemental analysis by characteristic X-rays can be carried out. These X-rays are emitted by the sample after electron bombardment as the electrons fall to a less excited states within the molecules.]

Figures 6 and 7 likely represent more charcoal, although it appears as though the surface might be covered with the rounded particle clusters characteristic of soot. It looks like the particles are coated with a film, which would indicate that not all of the kerogen was removed during oxidation. The irregularity of shape eliminates the possibility that the cluster is undissolved minerals.

Figure 8 is a picture of soot particles still attached to a mineral or possibly a piece of kerogen. These clusters have the characteristic morphology of soot, a group of rounded particles welded into a grapelike configuration (Figures 12a and 12c). Figures 9 and 10 show close up views of the particles. As can be seen in the photos, The rounded morphology is indeed present, particularly in Figure 10. Additionally, the irregular groupings eliminate the possibility of undissolved mineral in these specific areas.

Additional time was spent on trying to find isolated particles of soot. Figure 11 represents two or three isolates clusters of soot. Each grouping has highly rounded and irregular particles grouped together. On the right these particles are bunched together in a grape bunch-like form. Upon comparison to a standard of carbon black (Figures 12a and 12c, Wolbach *et al.*, 1989), it can be seen that the clusters possess soot like characteristics in the grouping of the particles.

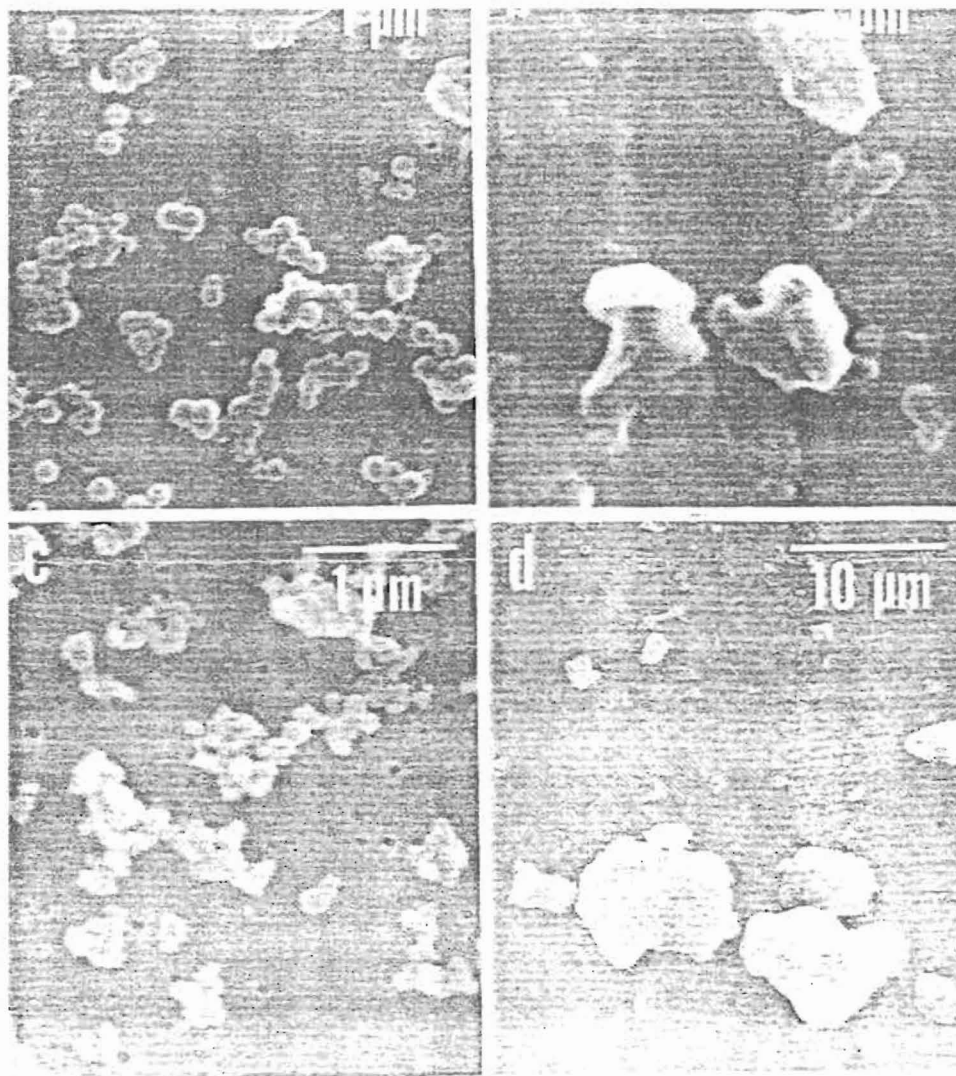


Figure 12. Carbonaceous residue from KT boundary clay at Woodside Creek, before (b) and after (a) oxidation. Soot can be seen in (a) when compared to Carbon black, unetched (c). Charcoal can be seen in (d). (Wolbach *et al.* 1989).

Comparison of relative soot to non-soot areas in a representative SEM micrograph of the sample was used to better estimate the approximate soot concentration in sample KT. Figure 8 was somewhat arbitrarily chosen as representative. Comparing the areas of soot (9.0 cm x 3.0 cm) in Figure 8 to the non-soot area (7.0 cm x 4.5 cm ) gives a soot to non-soot ratio of 27:32 or 9:11. This reduces the estimated KT soot concentration from 344 ppm to 155 ppm (Table III).

Table III. Corrected soot upper limit concentrations of the core samples

Sample	Upper limit concentration of soot (ppm)
KT	155
K50	46
T120	7

\*Concentrations good to one significant figure

### Discussion of Core Results.

The finding of soot in the sample lends credibility to the theory of worldwide distribution of soot. Massive wildfires on land and high winds, both caused by the impact of the giant meteorite, caused a large amount of soot to be distributed world wide. The presence of soot in the deep sea core sample indicates that carbon, both charcoal and soot, from fires indeed was carried to the ocean by winds. Runoff from the continental margins would not have produced soot deposition at this location. Soot and charcoal must have been blown into the atmosphere and carried by the high winds over the oceans. This material in the atmosphere could have blocked the photosynthesis of plankton, thereby contributing to an extinction in the sea as well.

## Results from Kara Ust-Kara Samples

Post-oxidation carbon residue concentrations were determined (Table IV).

Table IV. Concentration of soot in Kara Ust-Kara samples

Sample	Height of sample w/r/t top of suevite layer	Weight before demineralization (g)	Weight before oxidation (g)	Weight after oxidation (g)	Concentration of carbon (ppm)
SA1-604.16	2.4 m above	9.92519	0.10426	0.04393	4426
SA2-607.3	1.5 m above	10.23017	0.14119	0.02316**	4528†
SA2-015.0	2 cm above	9.81600	0.15085	0.04736	4824
SA1-009.0	0.1 m below	11.79752	0.18275	0.07979	6763
SA1-317.0	10 m below	9.78545	0.03645*	0.00981*	2005†
SA1-313.0	25 m below	10.43224	0.14227	0.09233	8850
SA1-311.5	30 m below	10.45373	0.09856	0.03555	3401

\*1/2 of sample SA1-317.0 was lost due to a cross contamination accident.

\*\*1/2 of sample SA2-607.3 was lost due to a breakage while changing the dichromate.

†Sample SA1-317.0 and SA2-607.3 weights were doubled due to the mass loss in order to give approximate soot concentrations.

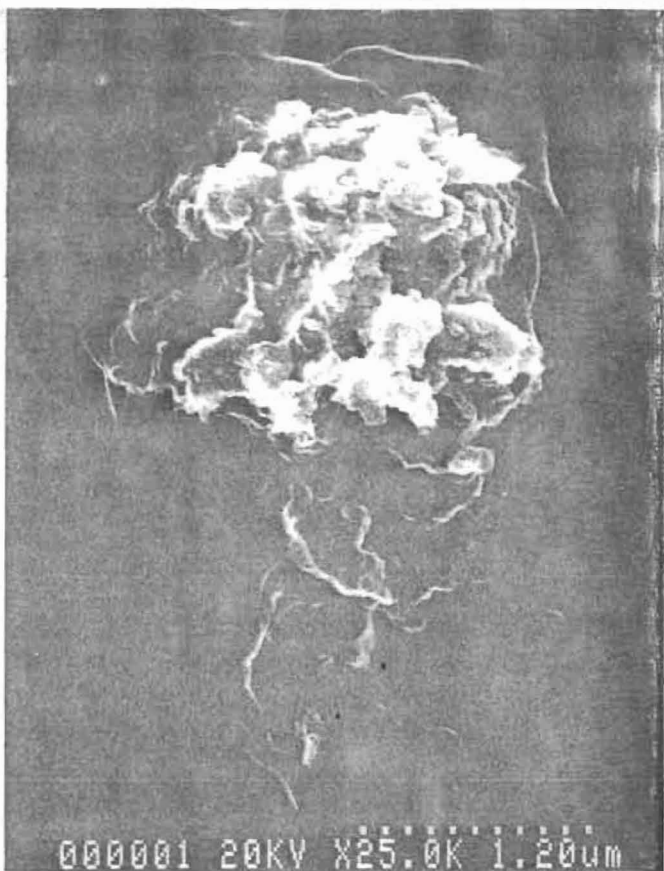


Figure 13. Soot particles clustered on top of charcoal (SA1-009.0).

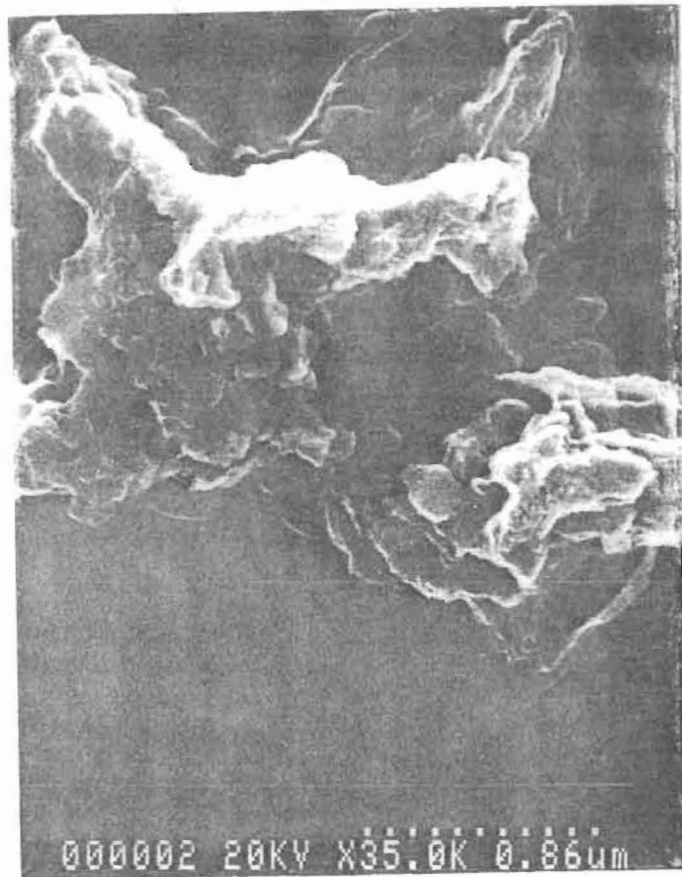


Figure 14. Soot particles clustered on top of charcoal (SA1-009.0).

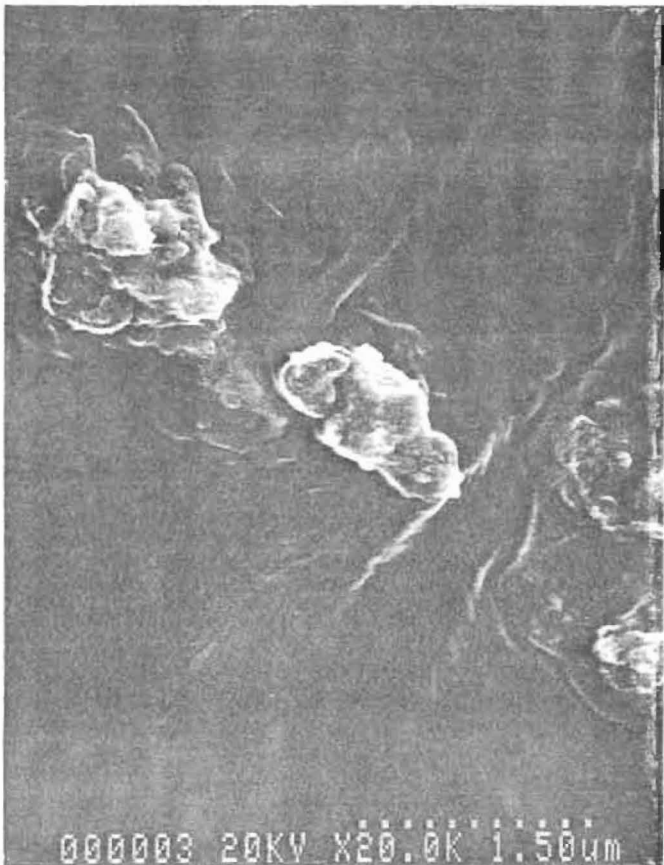


Figure 15. Charcoal (SA1-313.0).

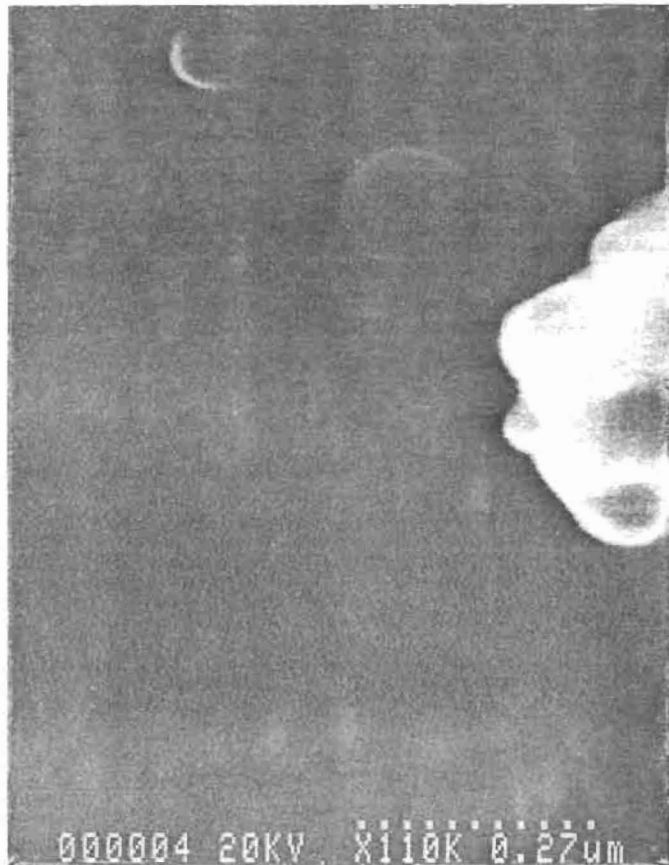


Figure 16. Soot cluster (SA2-015.0).



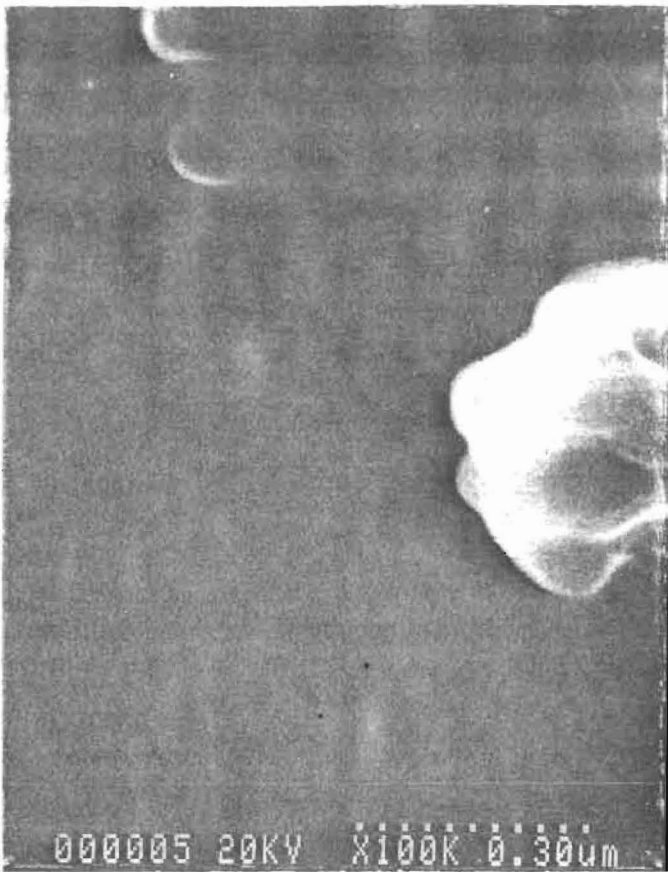


Figure 17. Soot cluster (SA2-015.0).

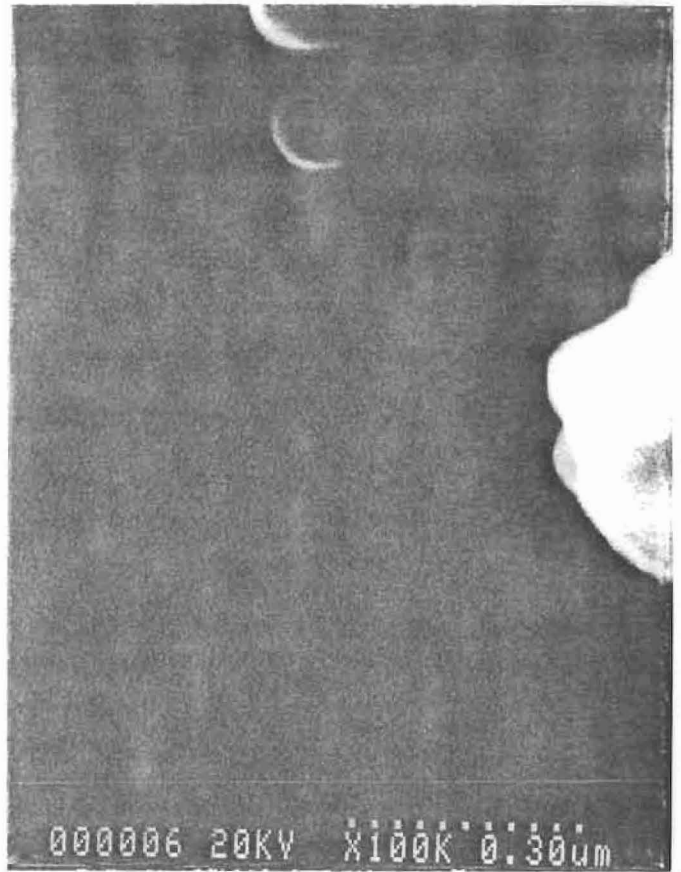


Figure 18. Soot cluster (SA2-015.0).

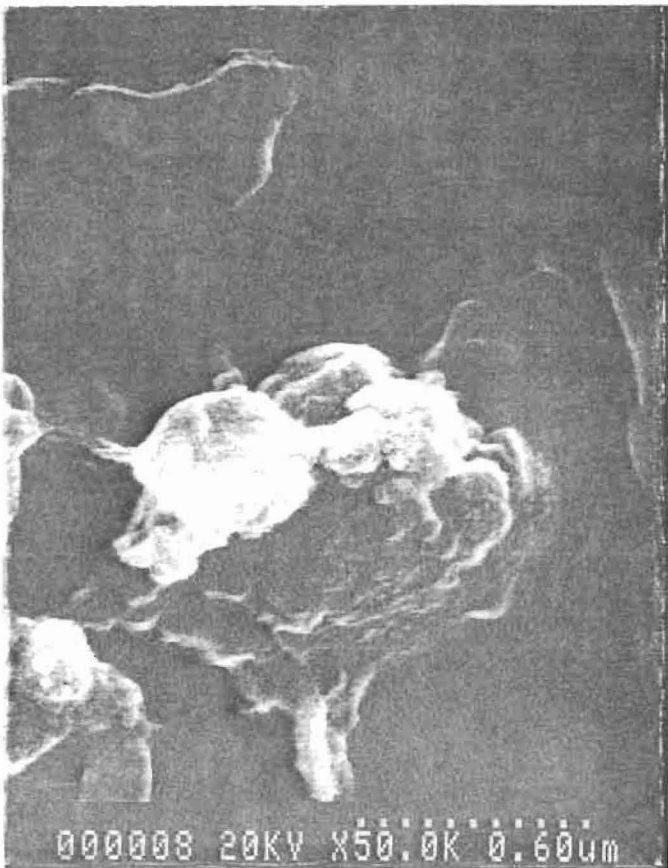


Figure 19. Soot attached to charcoal (SA2-607.3).



Figure 20. Soot attached to charcoal (SA2-607.3).



Figure 21. Isolated soot cluster (SA1-311.5).

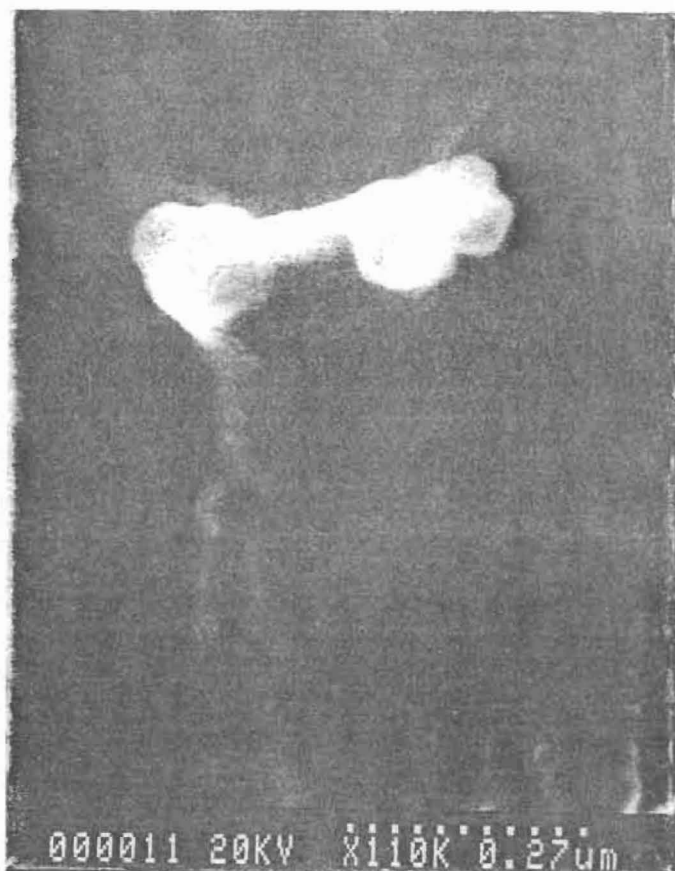


Figure 22. Isolated soot cluster (SA1-311.5).

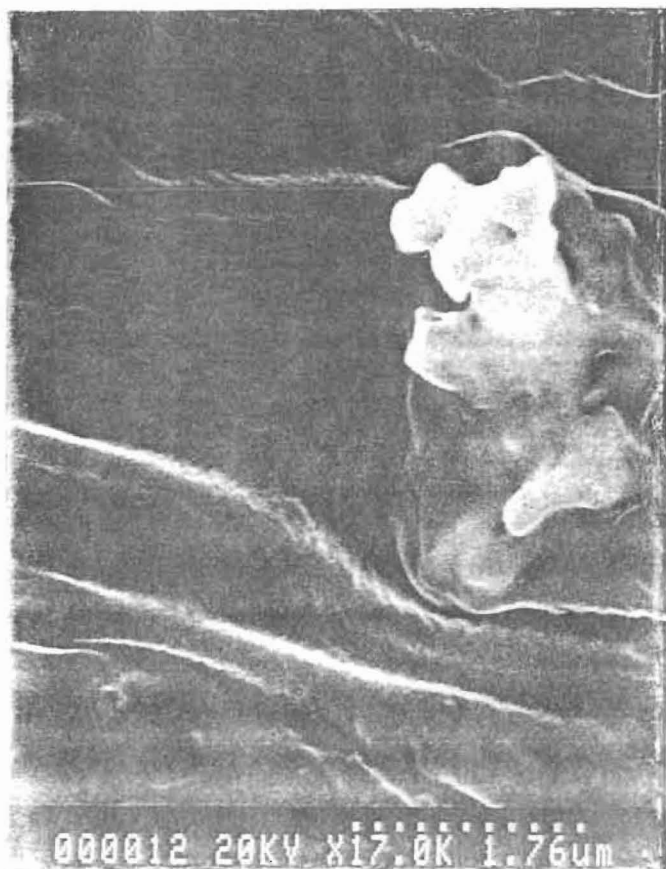


Figure 23. Soot w/ kerogen covering (SA1-317.0).

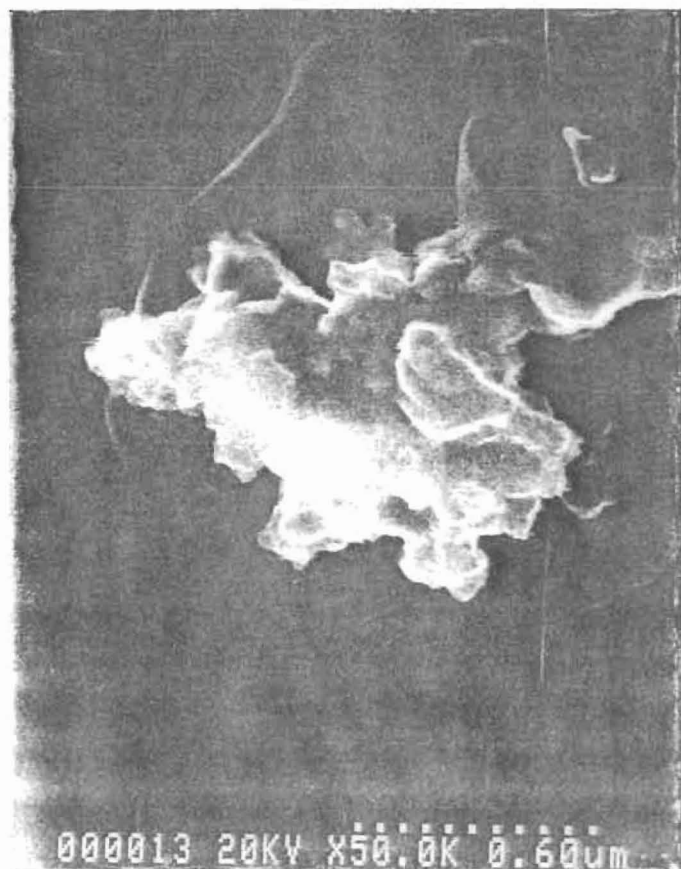


Figure 24. Soot under layer of kerogen (SA1-604.16).

Analysis of the Kara Ust-Kara samples under the Hitachi SEM confirmed the presence of soot in all of the samples. Figures 13 and 14 show soot particles, with their characteristic morphology, clustered together on top of charcoal. Charcoal can be seen in Figure 15. Figure 16-18 are micrographs of soot in sample SA2-015.0. Notice the rounded clusters in Figure 18. They are attached to one another in a distinct cluster. Figures 19 and 20 show soot attached to larger charcoal. Further oxidation of sample SA1-607.3 is required to give better definition of the soot. Figures 21 and 22 show an isolated cluster of soot particles at very high magnification. As with Figure 18, the rounded almost spherical clusters of soot are immediately recognizable. Figure 23 shows soot clusters which are still layered by the long-lived Type III kerogen. Further oxidation gives better definition of the soot clusters. Figure 24 again shows soot under kerogen. Table V summarizes the results in order of height above and below the top of the suevite layer.

Table V. Kara Ust-Kara results.

Sample	Height above and below top of suevite layer	Figure number	Charcoal and soot detected?
SA1-604.16	2.4 m above	24	Yes
SA2-607.3	1.5 m above	19-20	Yes
SA2-015.0	2 cm above	16-18	Yes
SA1-009.0	10 cm below	13-14	Yes
SA1-317.0	10 m below	23	Yes
SA1-313.0	25 m below	15	Yes
SA1-311.5	30 m below	21-22	Yes

## Discussion of Kara results

The presence of soot in all of the layers studied provides ample evidence for the theory of fires ignited by the impact. After oxidation all of the sample residues were blackened, a characteristic of a large concentration of soot and charcoal. However, since these samples were rather large, further oxidation is required for all of the samples in order to give better definition of soot in the micrographs. Soot presence both above and below the top of the suevite breccia indicates that some of the soot produced from the fires must have formed dense clusters which settled out with the heavier ejecta and charcoal. The presence of soot in the overlying sediments indicates that either the soot remained aloft and settled out slowly following impact, or else the soot traveled some distance before settling, then was carried to the topographic low of the crater by later runoff.

Soot was expected to be found in greatest concentrations near the top of the suevite breccia layer, due to the difference in the Stokes settling rates during deposition. Soot, a material of lesser density (approximately  $0.2 \text{ g/cm}^3$ ) than the suevites, was expected to settle out after the denser suevites. The results are consistent with this expectation, as the carbon residue concentrations are 4824 ppm at 2 cm above the top of the suevite breccia, and 6763 ppm at 0.1 m (10 cm) below the top of the suevite layer.

Following the initial post-impact carbon deposition, additional carbon runoff from land would continue to accumulate, but at decreasing rates and concentrations with time. This is observed in the steady carbon concentration decline from 10 cm below the top of the suevite breccia to 2.4 m above the top of the suevite layer.

Below the suevite layer, an interesting thing was observed: the carbon concentration increases markedly 25 m below the top of the layer to 8850 ppm. This might be explained in terms of composition: charcoal carbon has a density greater than that of soot ( $2.5 \text{ g/cm}^3$  vs.  $0.2 \text{ g/cm}^3$ ). Suevites have a density greater than  $2.0 \text{ g/cm}^3$ . Thus a large abundance of charcoal might have settled at about the same rate as some of the larger suevites, followed by lighter suevites and then the still lighter soot. If this could be confirmed, this would lend credence to the observation that charcoal

is typically deposited near the site of a fire, while soot is carried to some distance by winds. Thus near the fire, charcoal concentrations were expected to be greater than soot concentrations, while at a distance, soot dominates.

This theory could not be confirmed due to the presence of soot and charcoal in all of the samples. Charcoal presence in all of the Kara Ust-Kara samples indicates that fires occurred near the site of the impact. Charcoal settled out in all of the layers due to varying weights and runoff. Soot presence in all of the samples indicate that fallout with the larger suevites occurred in addition to runoff. This can be explained by the fact that soot, while in the air, possesses a slightly negative charge, while glassy suevites have a slightly positive charge. It is possible that electrostatic forces drew the soot and the heavier suevites together. Soot would therefore settle out further beneath the layer.

The marked increase 25 m below the top of the layer also might be explained in terms of stage of oxidation of the samples. After 600 hours, the dichromate solution continued to be consumed, as is evidenced by continual production of  $\text{Cr}^{3+}$  indicating that the samples still contained some form of kerogen. Since kerogen content were high in several of the samples, the weights and concentrations of elemental carbon are too large. Nevertheless, the qualitative observations above (Figures 13-24) can be made from the SEM micrographs.

The presence of soot and charcoal in all of the samples suggests that the fire was very close to the craters, and thus that the fires were ignited by the impact.

## Future Work

Future work on the core samples is necessary. A larger sample size should increase the chances of getting a verifiable weight for the residue which clearly contains soot. Furthermore, elemental analysis using characteristic X-rays in the SEM should be performed, using a non-carbon conductive tape which would allow the analysis of carbon in the sample. An elemental analysis would further aid in the identification of elemental carbon and confirm the presence of soot.

Further oxidation of all samples is necessary, as many of the samples appeared to still be reacting actively with the dichromate at the time oxidation was stopped. Additionally, samples SA1-317.0 and SA2-607.3 should be re-examined due to the mass loss, for an accurate determination of the soot concentrations within these two samples.

## References.

- Alekseev, A. S., S. B. Simirnova, M. A. Nazarov, and D. D. Badjukov. Paleontological age of the Kara impact Event. *Lunar and Planetary Science*, **XX**, pp. 5-6, 1988.
- Alvarez, L. W., W. Alvarez, F. Asaro, and H. V. Michel. Extraterrestrial Cause for the Cretaceous-Tertiary Extinction. *Science*, **208**, 4448, pp. 1095-1108, 1980.
- Alvarez, W. Toward A Theory of Impact Crises. *Eos*, **67**, 35, pp. 649, 653-655, 658, 1986.
- Badjukov, D. D., M. L. Bazhenov, and M. A. Nazarov. Paleomagnetism of Impactites of the Kara Impact Crater: Preliminary Results. *Lunar and Planetary Science*, **XX**, pp. 34-35, 1988.
- Bohor, B. F., E. E. Foord, P. J. Modreski, and D. M. Triplehorn. Mineralogic Evidence of an Impact Event at the Cretaceous-Tertiary Boundary. *Science*, **224**, 867, 1984.
- Koeberl, C., V. L. Sharpton, A. V. Murali, K. Burke. Kara and Ust-Kara Impact Structures (USSR) and their Relevance to the K/T Boundary Event. *Geology*, **18**, pp. 50-53, 1990.
- Masaitis, V. L., M. S. Mashchak, and B. A. Ivanov. Kara and Ust-Kara Craters Formed at the K-T Boundary by Low-Density Projectile. *Abstracts of Papers Submitted to the Eighth Soviet-American Microsymposium*, pp. 61-62, 1988.
- McLaren, D. J., and W. Goodfellow. Geological and Biological Consequences of Giant Impacts. *Annual Review of Earth and Planetary Science*, **18**, pp. 123-71, 1990.
- Nazarov, M. A., E. M. Kolesnikov, D. D. Badjukov, and V. L. Masaitis. Potassium-Argon age of the Kara Impact Event. *Lunar and Planetary Science*, **XX**, pp. 766-767, 1988.



- Smit, J., and G. Klaver. Sanidine Spherules at the Cretaceous-Tertiary Boundary Indicate a Large Impact Event. *Nature*, **292**, 47, 1981.
- Wolbach, W. S., E. Anders. Elemental Carbon in Sediments: Determination and Isotopic Analysis in the Presence of Kerogen. *Geochimica et Cosmochemica Acta*, **53**, pp. 1673-1647, 1989.
- Wolbach, W. S., E. Anders, M. A. Nazarov. Fires at the K/T Boundary: Carbon at the Sumbar, Turkmenia, Site. *Geochimica et Cosmochemica Acta*, **54**, pp. 1133-1146, 1990.
- Wolbach, W. S., I. Gilmour, E. Anders, C. J. Orth, and R. R. Brooks. Global fire at the Cretaceous-Tertiary Boundary. *Nature*, **334**, pp. 665-669, 1988.
- Wolbach, W. S., R. Lewis, E. Anders. Cretaceous Extinctions: Evidence for Wildfires and Search for Meteoric Material. *Science*, **230**, pp. 167-170, 1985.